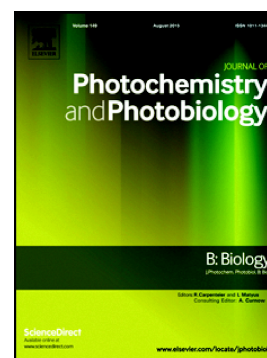


Journal Pre-proof

Silver nanoparticles doped TiO₂ catalyzed Suzuki-coupling of bromoaryl with phenylboronic acid under visible light

Yuning Chen, Li Feng



PII: S1011-1344(19)31596-9

DOI: <https://doi.org/10.1016/j.jphotobiol.2020.111807>

Reference: JPB 111807

To appear in: *Journal of Photochemistry & Photobiology, B: Biology*

Received date: 21 November 2019

Revised date: 4 January 2020

Accepted date: 24 January 2020

Please cite this article as: Y. Chen and L. Feng, Silver nanoparticles doped TiO₂ catalyzed Suzuki-coupling of bromoaryl with phenylboronic acid under visible light, *Journal of Photochemistry & Photobiology, B: Biology*(2019), <https://doi.org/10.1016/j.jphotobiol.2020.111807>

This is a PDF file of an article that has undergone enhancements after acceptance, such as the addition of a cover page and metadata, and formatting for readability, but it is not yet the definitive version of record. This version will undergo additional copyediting, typesetting and review before it is published in its final form, but we are providing this version to give early visibility of the article. Please note that, during the production process, errors may be discovered which could affect the content, and all legal disclaimers that apply to the journal pertain.

© 2019 Published by Elsevier.

Silver nanoparticles doped TiO₂ catalyzed Suzuki-coupling of bromoaryl with phenylboronic acid under visible light

Yuning Chen, Li Feng*

School of Civil and Transportation Engineering, Guangdong University of Technology, No100, Waihuan Xi Road, Guangzhou, Higher Education Mega Center, Panyu District, Guangzhou-510006, Guangdong, China.

*Corresponding author. Tel: +86-13594617802; fax: +86-02039322515

E-mail: fl19860314@126.com (L. Feng).

Abstract

The formation of the carbon-carbon bond in the synthetic chemistry explored in many ways. Suzuki-cross coupling is one of the ways to make bonds between two carbon atoms of similar molecules or different molecules. C-C bond was successfully formed between two aryl rings of aryl halides and phenylboronic acid at room temperature and atmospheric pressure under the visible illuminance. In this work we report, an in-situ synthesis of silver nanoparticles doped TiO₂ nanoparticles (NPs) and studied its catalytic activity as an eco-friendly, simple, recyclable and efficient catalyst for one-pot Suzuki-coupling of bromoaryl with phenylboronic acid under visible light. Only, 45 mg of the catalyst resulted in a 98% conversion of *p*-ethyl bromobenzene with a 97% yield of *p*-ethyl biphenyl using toluene as the solvent in the presence of visible light at atmospheric pressure. The electron-donating groups (e.g., ethyl group) substituted bromobenzene resulted in the maximum yields than that of the substitution with the electron-withdrawing groups. The catalyst shown significant catalytic activity up to seven recycling runs without any loss. The doping of silver nanoparticles boosted the catalytic activity at titanium dioxide surface as well as inside the pores. The high surface area of the semiconductor support provides the sites for accommodated silver nanoparticles and shows enhanced reactivity towards the coupling

reaction of bromoaryl with phenylboronic acid. The as-synthesized catalyst was thoroughly characterized by XRD, TEM, EDX, XPS, FTIR, TGA, UV-vis, Raman and BET analysis. The high recyclability of the photocatalyst remarked the footprints in the C-C coupling reactions.

Keywords: Metal oxide; Supported nanoparticle; Photocatalysis; Cross-coupling.

1. Introduction

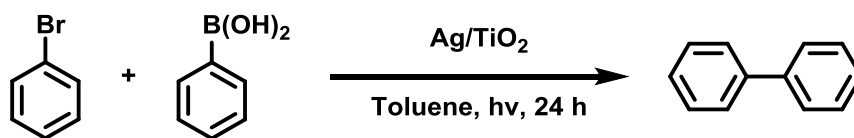
Cross-coupling is one of the promising approaches for making carbon-carbon single bond but has tedious protocols as developed [1]. It has versatile characteristics in a different field or organic chemistry, such as intermediates in natural products [2], bioactive compounds, etc. [3]. The coupling reaction occurred even at a high temperature $>100^{\circ}\text{C}$ due to the high activation energy barrier associated with the rate-limiting step [4]. The coupling of two carbon atoms is a challenging task explored in the last few decades [5]. The coupling reaction usually occurred with Palladium metal at high temperatures [6]. Other noble metals have been scrutinized to explore the coupled products. Akira Suzuki first reported Cross-coupling in the late 1970s over Pd-nanoparticles. He shared the noble prize with Richard F. Heck and Ei-ichi Negishi for their effort for the discovery and development of palladium-catalyzed cross couplings in organic synthesis. After the discovery, a plethora of research has been carried out over expensive noble metals and at high temperatures. The tedious recovery of homogeneous palladium metal and high cost limits the scope of the coupling reaction [7]. In the last few decades, the carbon-carbon coupling proved it as an essential approach to synthesize a variety of products in organic synthesis [8-11]. Support materials play crucial roles in synthetic chemistry. The efforts over cheap metal support materials for the accommodation of noble metals, such as nickel and copper to couple carbon-carbon atoms, have attracted the society.

High-temperature and high pressure darken the glow of the Suzuki coupling reaction. It requires a massive amount of energy to conduct the experiments. Also, the homogeneous catalysts have the drawbacks of separation and stability in the reaction for a long. An alternate, photocatalysis is a promising approach over thermal C—C coupling reactions due to their low cost of equipment [12]. The photocatalytic reactions proceeded through the radical-based mechanism driven by photogenerated electron-hole pairs at room temperature. Also, Suzuki-coupling reported in photocatalysis using homogenous as well as heterogeneous catalysts in the presence of visible light, but the recovery issue of the homogenous catalysts darkens their use in the coupling reactions. In this context, Li *et al.* reported the room-temperature Suzuki-coupling reaction over mesoporous carbon nitride supported Pd-nanoparticles a Mott-Schottky photocatalyst with a maximum of 99% yield of the coupled product under the visible illuminance [13]. Wang *et al.* reported Pd nanoparticle immobilized conjugated microporous polymer as a catalyst for the coupling of aryl halides with phenylboronic acid with 98% yield of the coupled product in the presence of visible light at room temperature [14]. Xiao *et al.* performed the coupling reaction of an aryl halide with phenylboronic acid over Au-Pd alloy with >99% yield of the coupled products in the presence of visible light [15]. Lao *et al.* synthesized the Mott-Schottky-type Pd/SiC catalyst for the coupling of aryl halide and phenylboronic acid under the visible illuminance [16]. Sun *et al.* reported the visible light assisted Suzuki-coupling reaction over Pd nanoclusters encapsulated inside the cavity of NH₂—Uio-66(Zr) MOF with >99% yield of the coupled product [17]. Xiao *et al.* carried the lower temperature cross-coupling reaction using palladium and gold alloy nanoparticles as the photocatalyst under the visible illuminance [18]. Koohgard *et al.* reported the plasmonic property and catalytic performance of Pd anchored to TiO₂ for Suzuki-Miyaura coupling in the presence of visible light [19]. Although, the above-reported protocols used the supports synthesized by tedious methods, such as

MOFs, graphene oxide form modified Hummer's method, which are very expensive and undesirable for the practical applications; cross-coupling is also being studied with silver nanoparticles and other supports synthesized from cheap transition metals, such as Ti, Ni, and Cu [20, 21]. However, silver doped nanoparticles have been used with a series of coupling reactions.

Recently, Yim et al. described the ultrathin WO_3 nanosheets supported PdO nanoclusters catalyzed C-C coupling under visible illumination [22]. Wang et al. performed the Suzuki-coupling reactions over graphitic carbon nitride supported palladium photocatalyst and got a TOF of 47.3 h^{-1} [23]. Sahoo et al. reported the visible-light assisted Suzuki-coupling using GO/LDH supported plasmonic AuPd bimetallic nanoalloy hybrid nanocomposite resulted in high yields of the corresponding biphenyls [24]. Although, silver doped catalysts have the advantage over the Pd-metal relatively less expensive and easily synthesized. Silver doped photocatalysts reported in a variety of coupling reactions [25]. In this regard, Sharma *et al.* reported $\text{Ag}@\text{Cu}_2\text{O}$ core-shell NPs as the catalysts applied to the Suzuki-cross-coupling reaction in the presence of visible light [26]. Gao *et al.* manufactured graphene oxide-palladium modified Ag-AgBr photocatalyst for cross-coupling of aryl halides and phenylboronic acid in the presence of visible light [27].

However, few reports are available with the first transition series metals supports. In this regard, based on the previous literature, we are focusing on low-cost metal supports, such as titanium, manganese, iron, cobalt, nickel, and copper for the Suzuki coupling in the presence of visible light. Herein, we report the most studied semiconductor TiO_2 as semiconductor support for the doping of Ag nanoparticles catalyzed cross-coupling of aryl halides and phenylboronic acid in the presence of visible light. We thought that this work would play an important role in the formation of carbon-carbon bond for the industrial point of view.



Scheme 1. Suzuki-coupling of bromobenzene and phenylboronic acid using Ag/TiO₂ under the visible illuminance.

2. Experimental section

2.1 Synthesis of Ag/TiO₂ photocatalyst

The desired photocatalyst was synthesized by the little modification in the method reported in the literature [28]. 5 mL of titanium tetrachloride solution was mixed with 5 mL of triethanolamine and 10 mL of ethanol at 0°C. Subsequently, the obtained white solid was dissolved in 50 mL of de-ionized water with continuous stirring for two h at room temperature. Silver nitrate (0.5-4 wt%) added to this homogeneous mixture and maintain the pH seven by the dropwise addition of ammonium hydroxide. The obtained precipitates were filtered, washed with distilled water by several times, followed by ethanol, and finally dried at 60°C for 24 h in a vacuum oven. The dried material was calcined at 550°C for four h in the presence of air in a muffle furnace. The as-synthesized catalyst was used for the photocatalytic reaction. For the comparative study, TiO₂ also prepared following a similar procedure without the use of silver salt.

2.2 Characterizations

UV-Vis absorption spectrum of the materials was recorded using a Perkin Elmer Lambda-19 UV-VIS-NIR spectrophotometer with a 10-mm quartz cell and BaSO₄ as a reference. X-ray diffraction (XRD) pattern was recorded to determine the crystallinity of the materials using Bruker D8 Advance diffractometer at 40 kV and 40 mA with Cu K_α radiation ($\lambda = 0.15418$ nm). Thermogravimetric analysis was carried out to find out the stability of the composites using a thermal analyzer TA-SDT Q-600. The thermal degradation pattern for the

materials was determined by thermogravimetric analysis in the temperature range of 40 to 800°C under nitrogen flow with a 10°C/min heating rate. Fourier transform infrared spectroscopy (FT-IR) used to determine the stretching and bending vibrations on a Perkin–Elmer spectrum RX-1 IR spectrophotometer having a potassium bromide window. All the samples were degassed at 200°C for three hours under an N₂ atmosphere. High-resolution transmission electron microscopy (HR-TEM) was used to analyze the nanocomposite and estimated the interplanar distances in the materials, using a JEM 2100 (JEOL, Japan) microscope. X-ray photoelectron spectroscopy (XPS) analysis was used to estimate the oxidation state and binding energy of elements in the composites using ESCA+ equipment (omicron nanotechnology, Oxford Instrument Germany) equipped with monochromator Aluminum Source (Al ka radiation $h\nu = 1486.7$ eV). ICP-AES was used to estimate the metal content in the final catalyst using Inductively Coupled Plasma Atomic Emission Spectrometer (ICP-AES, DRE, PS-3000J7, Leeman Labs Inc, USA). BET surface area, pore-volume, and mean pore diameter of composites were estimated using N₂ adsorption-desorption isotherm at 77 K by using Micromeritics ASAP 2010.

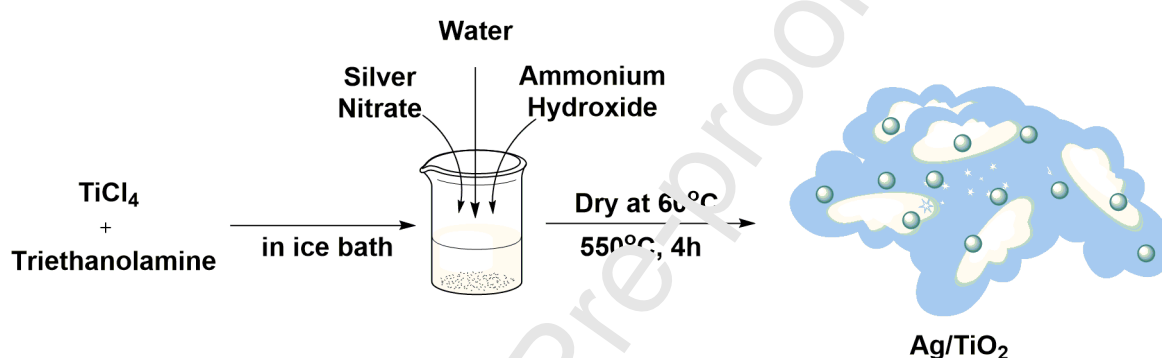
2.3 Photocatalytic experiment of Suzuki-coupling

Suzuki-coupling reaction was carried out in a 25 mL round bottom (RB) flask. Initially, RB was cleaned with water and then rinsed with acetone followed by drying at 60°C in an oven for one hour. One mmol of bromobenzene and two mmol of phenylboronic acid were poured into RB. Subsequently, 2 mL of toluene was inserted into the RB and closed with a rubber septum. The reaction solution was purged with N₂ gas for 30 min for the complete removal of air from the mixture. After that, RB was charged with 30 mg of Ag/TiO₂ photocatalyst, and the vessel was sealed with the rubber septum. The reaction mixture again purged with the N₂ gas for the residual air and then irradiated with the 20 W white LED ($\lambda \sim 420$ nm) for 24 h. The sample was analyzed with TLC after every two-hour interval. The conversion and the

yield were determined with GC-FID (Thermo equipped with Stabilwax® w/Integra- Guard® 30-meter-long column), and confirmation was obtained by the ^1H and ^{13}C NMR of the pure samples.

3. Results and Discussions

The photocatalyst was synthesized using silver nitrate and titanium tetrachloride as the precursor of silver and titanium. The synthesis of the photocatalyst was demonstrated in scheme 2.



Scheme 2. A synthetic protocol of Ag/TiO₂ from silver nitrate and titanium tetrachloride.

Crystallinity, crystal size, and phases of the materials were determined by X-ray diffraction spectroscopy (Figure 1). The diffraction pattern of TiO₂ indicated the characteristic diffraction peaks correspond to the anatase form of TiO₂, and the intensity of the diffraction peaks suggested that the materials were highly crystalline (Figure 1a). TiO₂ semiconductor has the tetragonal structure with a body-centered crystal lattice and follows the JCPDS Card No. 89-4921 [29]. The loading of the silver nanoparticles onto the TiO₂ semiconductor shows the signal of reduced AgNPs. 2%Ag/TiO₂ shows a diffraction peak at 44.22° for the reduced silver nanoparticles (JCPDS Card No. 89-3722) which corresponds to (200) plane (Figure 1b) [30]. The rest of the diffractogram remains as it is for TiO₂ semiconductor support. 4%Ag/TiO₂ also shows a diffraction signal at a similar angle for reduced Ag nanoparticles but in little bit enhanced intensity confirms the successful loading of the silver nanoparticles

at TiO₂ semiconductor support. This also reveals that the doping of the silver nanoparticles did not change the character and the crystal lattice of TiO₂ support (Figure 1c).

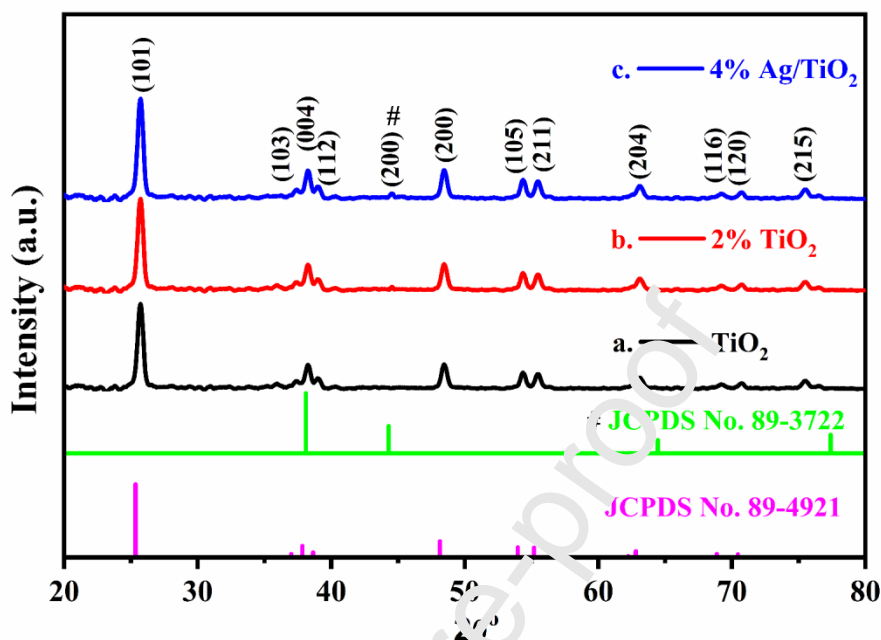


Figure. 1. X-ray diffractogram of (a) TiO₂, (b) 4% Ag/TiO₂ and (c) 4% Ag/TiO₂ photocatalyst synthesized and calcined at 550°C.

The stretching and bending vibrations of TiO₂, 2% Ag/TiO₂, and 4% Ag/TiO₂ photocatalyst were determined by the FT-IR technique using potassium bromide as reference material (Figure 2). The vibrational peak at 1078 cm⁻¹ corresponds to the characteristic Ti-O stretching in the crystal lattice of TiO₂ semiconductor (Figure 2a). The next two vibrations at 1450 and 1635 cm⁻¹ were due to the intercalated water molecule in the semiconductor support while the later broad signal obtained at 3391 cm⁻¹ attributed to the O-H stretching of the hydroxyl moieties suggested that the semiconductor absorbs moisture from the atmosphere [31]. This indicated that the oxygen atoms present at the surface of TiO₂ semiconductor are in the form of -OH groups. The insertion of silver nanoparticles in the semiconductor shows the vibrational signals in the spectra with 2% loading. The doping of 2% AgNPs onto TiO₂ semiconductor show slightly shifted stretching vibration with a shoulder at 1674 cm⁻¹

exhibited the Ag-O stretching reveals the incorporation of the silver nanoparticles in TiO₂ semiconductor (Figure 2b) [32]. Another signal at 3245 cm⁻¹ attributed to the Ag-OH stretching due to the moisture content in the final catalyst. Rest of the spectrum for 2%Ag/TiO₂ photocatalyst remains the same as for TiO₂ semiconductor. Further, loading of 4%AgNPs shows peaks similar to the 2% loading but the slightly increased intensity of the vibrational peaks indicating the higher loading of AgNPs in the nanocomposite (Figure 2c).

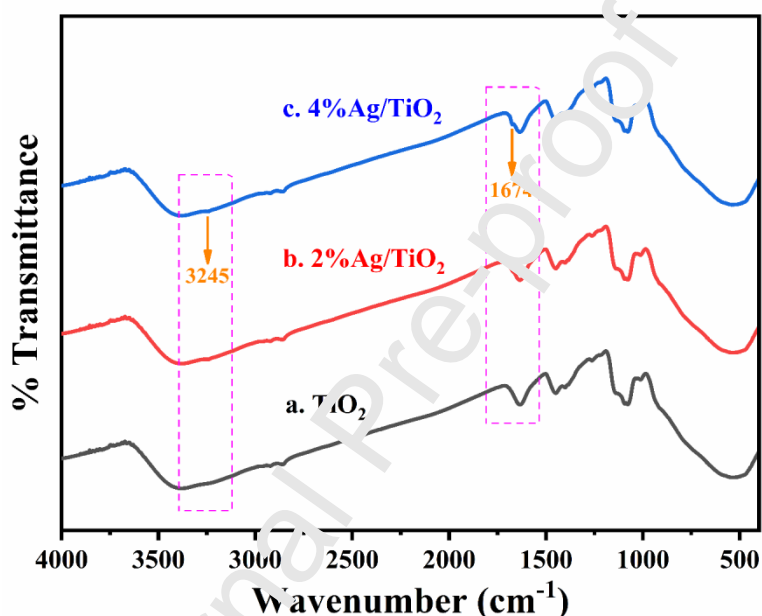


Figure. 2. Fourier transform infra-red (FTIR) spectra of (a) TiO₂, (b) 2%Ag/TiO₂ and (c) 4%Ag/TiO₂ using KBr as standard for the instrument.

The absorption maximum for TiO₂, 4%Ag/TiO₂, and 4%Ag/TiO₂ photocatalyst were estimated by UV-Vis spectrophotometer using barium sulfate as the standard (Figure 3). UV-vis spectrum of TiO₂ shows broadband in UV region 246-384 nm, indicating that the TiO₂ had strong absorption in the UV region, not in the visible region (Figure 3a) [33]. However, the doping of silver nanoparticles onto the semiconductor makes the nanocomposite capable of absorbing visible light. Loading of 2 wt% of AgNPs on TiO₂ shows a hump in the range between 400-500 nm along with the broad characteristic signal of Ag (Figure 3b) [34]. The

nanocomposite contains both the TiO_2 and AgNPs absorption confirms the successful incorporation. The absorption maximum of the nanocomposite in the visible region shows the activity for the visible-light-induced reaction. Higher loading, 4 wt% of AgNPs onto TiO_2 also exhibited similar hump at the same wavelength, but slightly high intensity suggested the more absorption with higher loadings of AgNPs (Figure 3c).

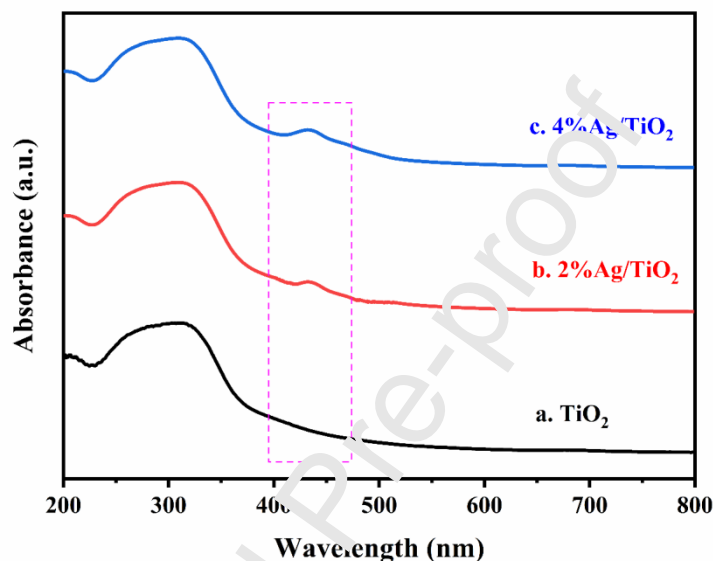


Figure. 3. Ultra-Violet-visible (UV-vis) spectra of (a) TiO_2 , (b) 2% Ag/ TiO_2 and (c) 4% Ag/ TiO_2 photocatalyst using BaSO_4 as the reference material.

HR-TEM images, SAED pattern, and EDX pattern for 2% Ag/ TiO_2 photocatalyst are demonstrated (Figure 4). The sample was prepared at a lacey carbon grid using ethanol as the solvent. The nanocomposite shows uniformly distributed granules at a 100 nm scale (Figure 4a). The doping of AgNPs onto TiO_2 observed in the nanocomposite where the silver nanoparticles lie in the range from 1.5-5 nm at 5 nm scale (Figure 4b) [35]. SAED pattern shows the clear, bright spots which confirm that the nanocomposite is crystalline (Figure 4c). The loading of the silver nanoparticles observed in the EDX pattern of the 2% Ag/ TiO_2 photocatalyst and found 1.87 wt%, which is close to 2% loading of silver nanoparticles.

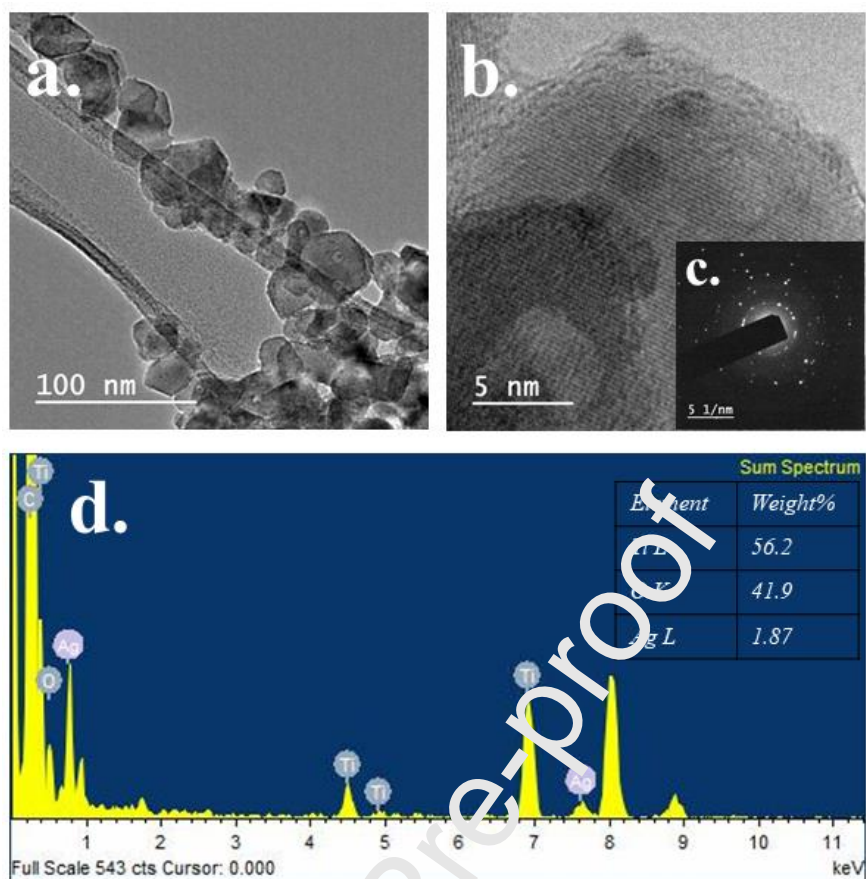


Figure 4. (a, b). HR-TEM images, (c) SAED pattern and (d) EDX pattern of 2% Ag/TiO₂ photocatalyst.

The electronic properties for TiO₂ and 2% Ag/TiO₂ photocatalyst were determined by Raman spectroscopy at wavelength 532 nm (Figure 5). Anatase TiO₂ shows five characteristic vibrational signals at 150, 201, 393, 509, and 633 cm⁻¹ attributed to the E_g, E_g, B_{1g}, A_{1g}/B_{1g}, and E_g Raman active modes and confirmed the tetragonal space group D_{4h} (Figure 5a) [36-39]. The doping of silver nanoparticles onto TiO₂ did not show any effect in 2% Ag/TiO₂ photocatalyst (Figure 5b). The lower doping of the silver nanoparticles onto TiO₂ semiconductor did not show any vibration along with the semiconductor support suggested that 2% Ag/TiO₂ photocatalyst did not change the electronic properties and behave as usual.

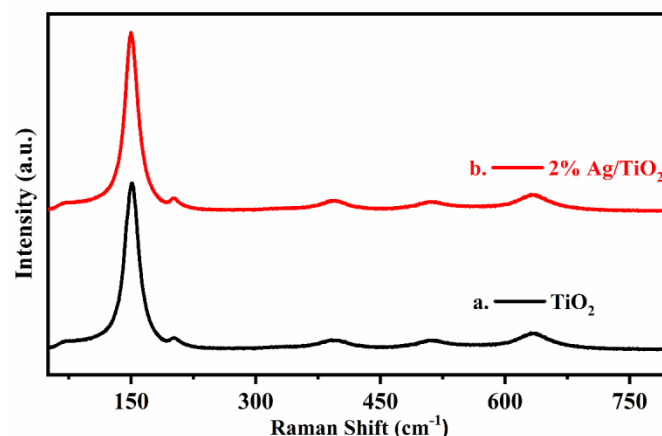


Figure 5. Raman frequencies of (a) TiO_2 and (b) 2% Ag/TiO_2 photocatalyst.

The surface chemical properties of 2% Ag/TiO_2 photocatalyst was determined by X-ray photoelectron spectroscopy (Figure 6). XPS spectra of Ag-3d shows two peaks for $3d_{3/2}$ and $3d_{5/2}$ attributed at 373.6 eV and 368.3 eV, respectively correspond to the metallic silver $\text{Ag}(0)$ in the 2% Ag/TiO_2 nanocomposite and free to bind with the oxygen atoms (Figure 6a). The metallic silver was in a good agreement with the literature reported by Paul et al. [40]. Also, XPS of Ti-2p exhibited two binding energies of 464.3 eV and 458.9 eV corresponds to the Ti- $2p_{1/2}$ and Ti- $2p_{3/2}$, respectively which suggested that the titanium is present in +4 oxidation state (Ti^{4+}) (Figure 6b) [41].

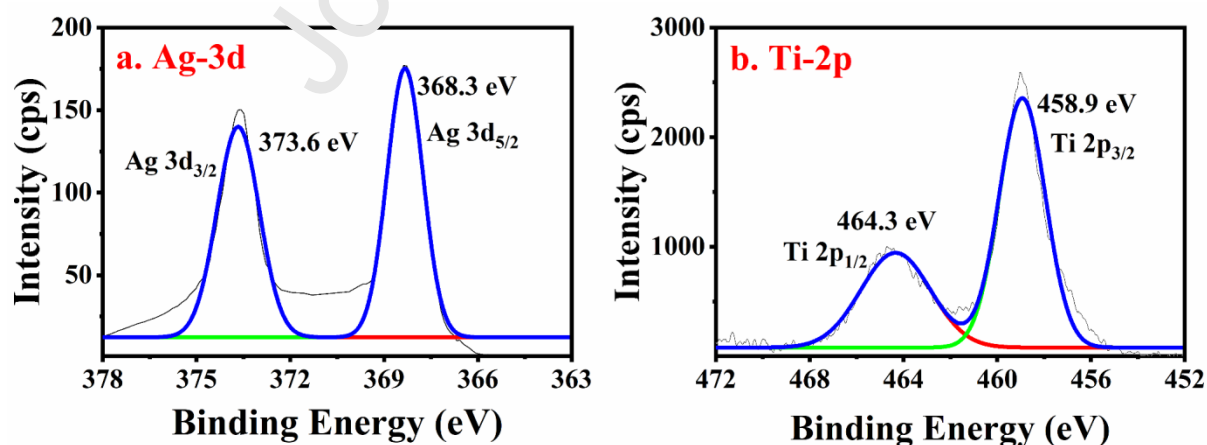


Figure 6. XPS analysis of (a) Ag-3d and (b) Ti-2p for 2% Ag/TiO_2 photocatalyst.

The BET surface area, pore-volume, and the average pore size were determined by the N₂ adsorption-desorption isotherm at -196°C (Figure 7). All the samples were degassed at 300°C for 3 h in the presence of N₂ gas. The N₂ adsorption-desorption isotherm for TiO₂ shows type IV isotherm with the H3 hysteresis loop (Figure 7a) [42]. The hysteresis of the isotherm and the pore size distribution reveals the mesoporous nature of TiO₂ semiconductor support. The surface area, pore diameter and pore volume determined for TiO₂ were 45 m²-g⁻¹, 13 nm, and 0.013 m³-g⁻¹. The average pore diameter of 13 nm lies in the mesoporous range of the pore and confirms the mesopores in the semiconductor. After deposition of 2 wt% silver nanoparticles onto the TiO₂ semiconductor, the N₂ adsorption-desorption isotherm neither changed from type IV nor changed the hysteresis loop from H3 (Figure 7b). The surface area of 2%Ag/TiO₂ nanocomposite decreased up to 29 m²-g⁻¹ due to the deposition of the silver nanoparticles at the surface of TiO₂. The average pore size decreased to 11 nm, but the pore volume slightly increased to 0.019 m³-g⁻¹ due to the deposition of the AgNPs into the pores of the semiconductor [43]. The decrement in the pore size of 2%Ag/TiO₂ photocatalyst does not influence the range of mesoporosity and remains intact as TiO₂ semiconductor. More loading, i.e., 4 wt% of AgNPs on TiO₂, reveals the similar N₂ adsorption-desorption isotherm and hysteresis loop as well. The increased loading of AgNPs slightly decreased the surface area (26 m²-g⁻¹) and average pore diameter (10 nm), but slightly increase pore volume (0.021 m³-g⁻¹) in a small extent (Figure 7c).

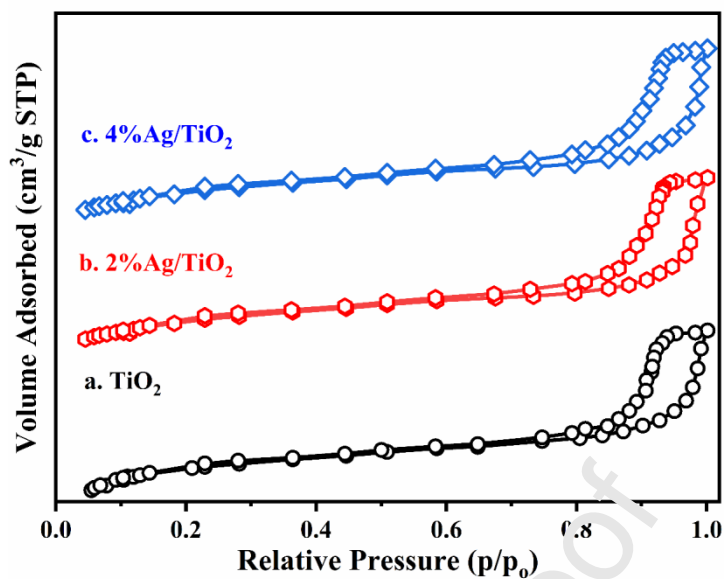


Figure. 7. N₂ adsorption-desorption isotherm of (a) 2%Ag/TiO₂, (b) TiO₂ and (c) silver nanoparticles (AgNPs).

The weight loss of TiO₂, 2%Ag/TiO₂, and 4%Ag/TiO₂ were determined by thermal gravimetric analysis (TGA) and derivative thermal analysis under N₂ atmosphere (Figure 8). The thermogram of TiO₂ exhibited 11% initial weight loss at 101°C attributed to the adsorbed water content from the atmosphere (Figure 8a). No weight loss occurred at a higher temperature and remained 89% of the semiconductor at 800°C, indicating the stability of TiO₂ [44]. The incorporation of AgNPs into the semiconductor slightly changes the thermal behavior 2%Ag/TiO₂ nanocomposite (Figure 8b). The initial weight loss (5%) occurred at 60°C for the evaporation of the water molecules. Further heating of the nanocomposite shows a steady loss of weight at 800°C and 84% of the material remains at the end of the analysis. On heating to 4%Ag/TiO₂, 5% weight loss occurred at 60°C, which corresponds to the evaporation of water at a lower temperature (Figure 8c). Further heating the material, 4% weight loss from 88-84 on the weight % scale found at 500°C was attributed to the elimination of nitrate precursor AgNPs [45]. This weight loss also supported by the DTA, shows a sharp

signal at 517°C corresponds to the weight loss at 500°C. The rest of the TGA shows small, steady loss of weight and 82% of total weight remained at 800°C.

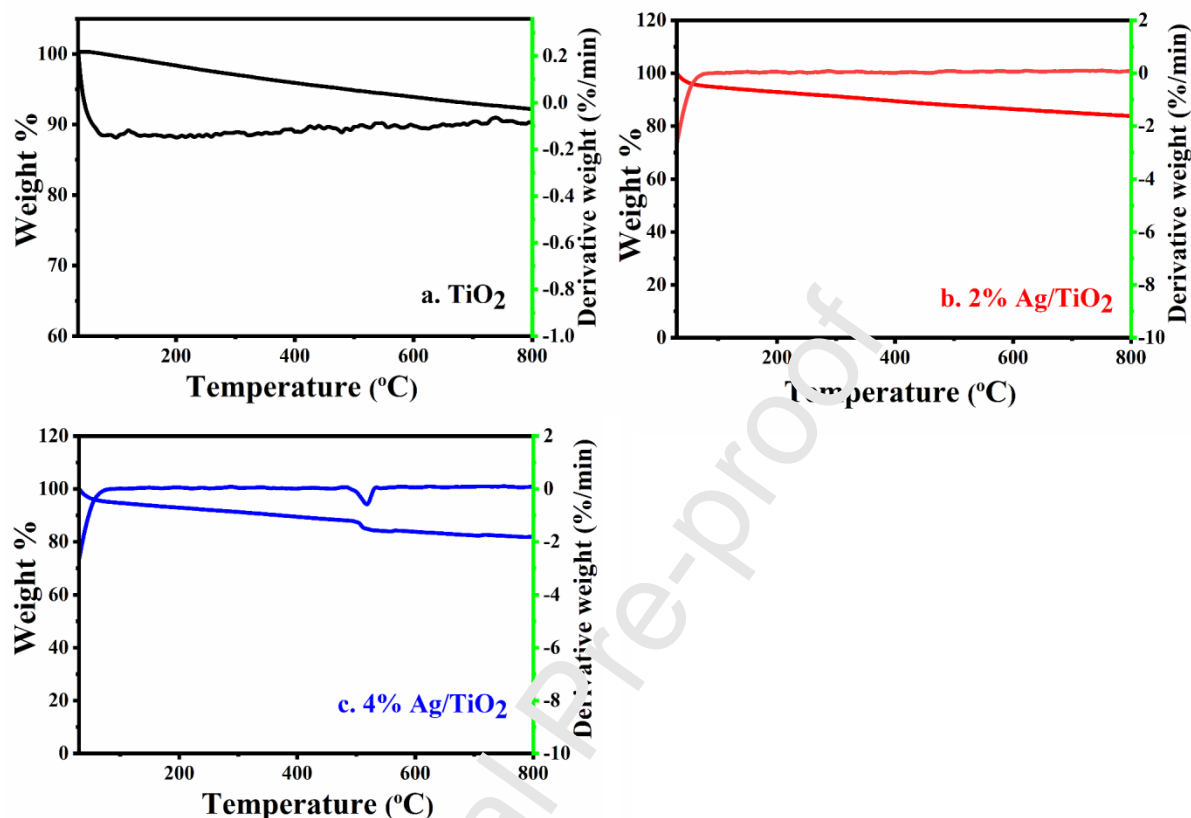


Figure 8. Thermogravimetric and derivative weight loss per min. for (a) TiO₂, (b) 2% Ag/TiO₂ and (c) 4% Ag/TiO₂ plotted against the temperature from 30-800°C under N₂ atmosphere.

Photocatalytic activity of the catalyst

The coupling reaction was performed in a 25 mL RB charged with bromoaryl, phenylboronic acid, toluene, and photocatalyst. The closed RB purged by N₂ gas for 30 min and then removed, followed by irradiation by white LED light. The catalyst was separated from the reaction mixture with the help of a syringe filter at the end of the reaction, and 1 μL of the reaction mixture was injected into the GC-FID to estimate the conversion and yield of the

substrate and the product, respectively. The products were further confirmed using ^1H and ^{13}C NMR spectroscopy.

Suzuki-coupling reaction was screened with variation in the loading of silver onto TiO_2 using different solvents at room temperature in the presence of visible light. At first, water was used as the reaction solvent for the coupling reaction using 2%Ag/ TiO_2 photocatalyst. The conversion of the substrate and yield of the product were moderate. While using ethanol as a solvent, a slight increase in the yield observed under the identical reaction condition. Like ethanol, similar results were obtained with acetonitrile shows that polar solvents poorly proceeded the coupling reaction. A significant increase in yield of the product was observed with DMF as the reaction medium up to 76 yields of the coupled product. Toluene, a less polar solvent efficiently converted bromobenzene into the corresponding coupled product in 92% yield, indicating that toluene is the suitable solvent for the Suzuki-coupling reaction. Further, to optimize the loading of silver onto TiO_2 , a variation from 0.5-3.0% loading of Ag studied for the reaction. Less loading of the noble metal shows the low efficiency of the catalyst under the identical reaction condition. 0.5%Ag/ TiO_2 shows the lowest yield of 52% of the product. An increase in the loading of Ag increased the efficiency of the reaction and afforded a higher yield. 2%Ag/ TiO_2 resulted in the highest 92% yield of the corresponding product in toluene while a further increase of Ag loading shows no effect or slightly decreases the yield of the product. In the absence of light, there was no product detected in GC-FID. The reaction proceeded at TiO_2 but gave poor results while no reaction was found in the absence of the photocatalyst. Commercial anatase and rutile TiO_2 used to compare with the synthesized anatase TiO_2 under similar reaction conditions, but the results were not as good as-synthesized TiO_2 .

Table 1. Optimization of parameters for the photocatalytic coupling of bromobenzene and phenylboronic acid.^a

Sr. No.	Catalyst	Solvent	Conv. (%)	Yield (%) ^b
1.	2% Ag/TiO ₂	Water	57	52
2.	2% Ag/TiO ₂	Ethanol	63	61
3.	2% Ag/TiO ₂	Acetonitrile	64	60
4.	2% Ag/TiO ₂	DMF	79	76
5.	2% Ag/TiO ₂	Toluene	95	92
6.	0.5% Ag/TiO ₂	Toluene	23	20
7.	1% Ag/TiO ₂	Toluene	53	51
8.	1.5% Ag/TiO ₂	Toluene	79	78
9.	2.5% Ag/TiO ₂	Toluene	94	91
10.	3% Ag/TiO ₂	Toluene	93	91
11.	3.5% Ag/TiO ₂	Toluene	89	88
12.	4% Ag/TiO ₂	Toluene	89	85
13. ^c	2% Ag/TiO ₂	Toluene	-	-
14.	TiO ₂	Toluene	11	09
15.	No catalyst	Toluene	-	-
16.	TiO ₂ (Commercial anatase)	Toluene	08	06
17.	TiO ₂ (Commercial rutile)	Toluene	05	04

^aReaction condition: Bromobenzene (1 mmol), phenylboronic acid (2 mmol), catalyst (45 mg), solvent 2 mL for 24 h, at room temperature, white light 20 W LED ($\lambda > 420$ nm). ^bIsolated yield by GC-FID. ^cNo light.

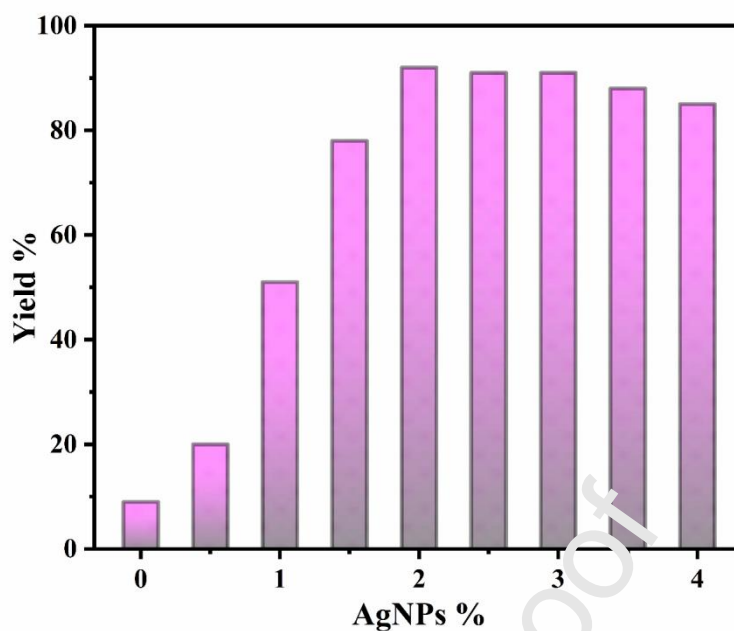
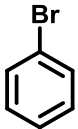
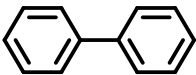
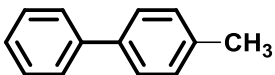


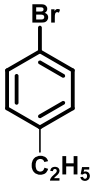
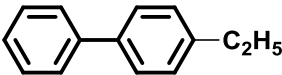
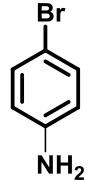
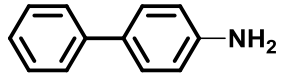
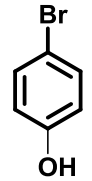
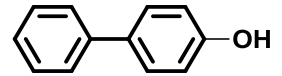
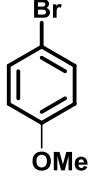
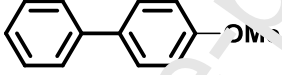
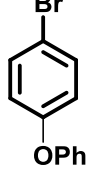
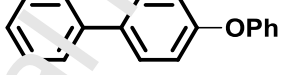
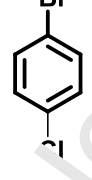
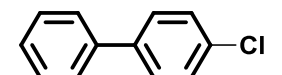
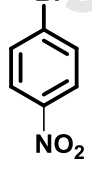
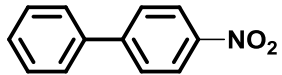
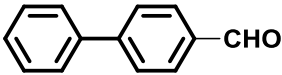
Figure. 9. A plot of yield % against the loading of AgNPs for the Suzuki-cross-coupling reaction.

The scope of the reaction was elaborated for the substituted bromoaryls under identical reaction conditions. 2% Ag/TiO₂ found to be the optimum photocatalyst for the coupling of bromoaryl and phenylboronic acid in the presence of visible light. Bromoaryls with electron-donating groups at *para* position afforded the excellent yield than the non-substituted bromobenzene up to 97% yield of the corresponding product (entry 2-3). *p*-methyl bromobenzene resulted in a 95% yield of 4-methyl-1,1'-biphenyl (entry 2). Substitution of an ethyl group at *para* position enhanced the efficiency and gave 97% yield of 4-ethyl-1,1'-biphenyl (entry 3). The substitution of electron-withdrawing groups at the *para* position in bromobenzene retarded the yield of the corresponding coupled biphenyl compounds up to 83% (entry 4-10). Bromobenzene with amino substitution at a *para*-position slightly reduced the yield of 94% for (1,1'-biphenyl)-4-amine (entry 4). This decrease also found in *para* hydroxy-substituted bromobenzene afforded a 91% yield of (1,1'-biphenyl)-4-ol (entry 5). While the methoxy-substituted bromobenzene provided higher yield 94% of 4-methoxy-1,1'-

biphenyl due to the electron-donating methyl group at the oxygen of the methoxy group (entry 6). Phenoxy substituted bromobenzene further reduced the yield of 4-phenoxy-1,1'-biphenyl about 93% indicating that the conjugated phenyl ring slightly restricts the product formation. Highly electronegative and strong electron-withdrawing groups resulted in the lowest yield amongst the substrate used. Chloro-substituted bromobenzene gave a 90% yield of 4-chloro-1,1'-biphenyl due to the high electronegativity of chlorine (entry 8). Strong electronegative NO₂ substituted bromobenzene afforded much lower yield 83% of 4-nitro-1,1'-biphenyl suggested that the electron pulling tendency of nitro group slightly retards the coupling of phenyl rings of 4-bromo nitrobenzene and phenylboronic acid. Further, 4-bromo benzaldehyde afforded somehow 87% yield of (1,1'-biphenyl)-4-carbaldehyde showing better efficiency than the product yield of 4-nitro-1,1'-biphenyl. The overall summary found that the biphenyls with electron-donating groups at *para* position show excellent activity than that with electron-withdrawing groups for the Suzuki-coupling of substituted bromoaryls and phenylboronic acid in the presence of visible light.

Table 2. Suzuki-coupling of bromoaryls and phenylboronic acid under the optimized condition.

Sr. No.	Substrate	Product	Conversion (%) ^b	Yield (%) ^c
1.			95	92
2.			96	95

3.			98	97
4.			97	94
5.			95	91
6.			96	94
7.			93	90
8.			91	90
9.			87	83
10.			89	87

^aReaction: 1 mmol of Substrate, 2 mmol of phenylboronic acid, 45 mg of photocatalyst, 2 mL of toluene, reaction time 24 h, 20 W white LED ($\lambda > 420$ nm), room temperature. ^bConversion by GC-FID. ^cIsolated yield by GC-FID.

Further, the photocatalyst was recycled after the completion of the cross-coupling reaction. The photocatalyst was separated by filtration, thoroughly washed with ethanol for the complete removal of toluene through the centrifugation, and dried in a vacuum oven at 60°C for 24 h. The recycled photocatalyst was reused for the coupling reaction up to seven times with a small or negligible loss of activity (Figure 10). This shows that the recovered photocatalyst was highly efficient and productive for the coupling reactions.

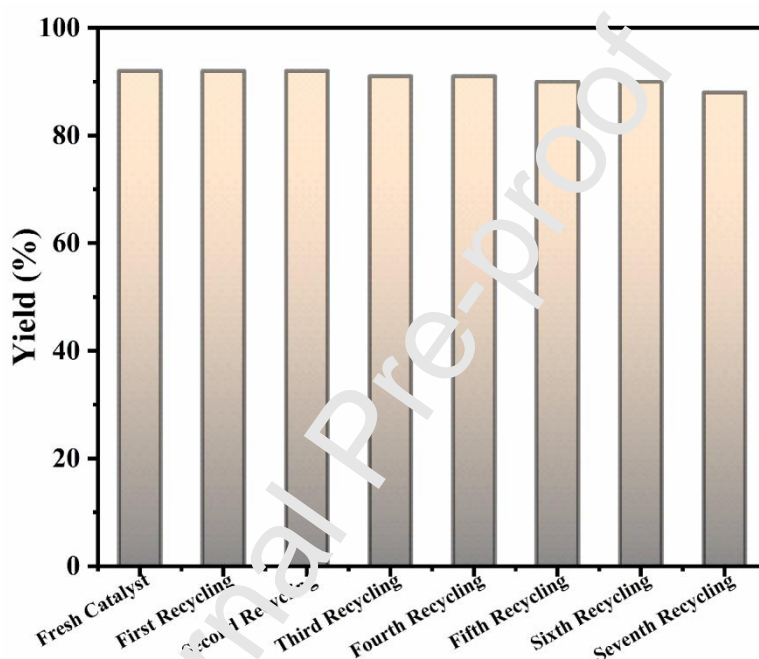


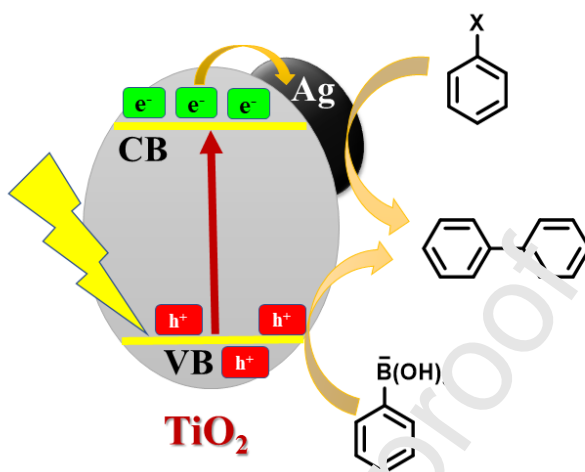
Figure. 10. A plot of yield against the recovered catalysts in each cycle for the Suzuki-cross-coupling reaction.

Furthermore, the superiority of the developed protocol established by the comparison of the already reported literature for the Suzuki-coupling reactions based on the silver doped photocatalysts in the presence of visible-light in Table 3. The table showed that the highest coupled biphenyls obtained with Ag/TiO₂ photocatalyst reported in the present report. The main advantage of the catalytic system is that there was no use of base or the reaction proceeded without the co-catalyst.

Entry	Photocatalyst	Base	Time (h)	Yield (%)	Ref.
1.	Pd/Ag/SBA-15	K ₂ CO ₃	2	80	Verma et al.[46]
2.	Ag@Cu ₂ O	K ₂ CO ₃	12	89	Sharma et al.[26]
3.	Ag/TiO ₂	-	24	97	This work

The mechanism of the Suzuki-coupling reaction is well established. However, here we have proposed the mechanism for coupling of substituted bromoaryls and phenylboronic acid using Ag/TiO₂ as a photocatalyst in the presence of visible light. TiO₂ is an excellent known photocatalyst in the photocatalysis and mostly studied for maximum reactions. TiO₂ alone is UV-active as well as shows moderate activity in the presence of visible light but, the doping of noble metal nanoparticles makes it a suitable catalyst for the photo-responsive reaction [47-49]. The noble metal nanoparticles show plasmonic resonance through which the electrons are quickly transferred to the molecule which has to be reduced. Silver nanoparticles showed the plasmonic resonance through which the yield of the biphenyls increased. In the presence of visible light, TiO₂ semiconductor alone performs small excitation of the electrons from the valence band (VB) to conduction band (CB) in the visible light. In combination with the silver nanoparticles, the combined photocatalyst 2%Ag/TiO₂ shown activity towards the coupling reactions. The excitation of electrons enhanced by the doping of AgNPs. The electrons of VB of TiO₂ get excited to CB in the presence of visible light and produced electrons and holes. These holes utilized to oxidize the quaternary phenylboronic acid at VB and generated the phenyl radical. The excited electrons of CB then

transferred to the silver nanoparticles, where the silver nanoparticles utilized these electron through plasmonic resonance for the aryl halides [50]. Then, both the species react with each other and generated the biphenyls as the coupled product.



Scheme. 3. A plausible mechanism of the Suzuki coupling reaction catalyzed by 2% Ag/TiO₂ photocatalyst in the presence of visible light.

4. Conclusion

Suzuki-coupling of bromoaryls has been successfully carried out using Ag/TiO₂ catalyst under the visible illuminance. Ag/TiO₂ photocatalyst exhibited the superior efficiency for coupling of bromoaryls with phenylboronic acid into the corresponding bi-aryls up to 98% yield in toluene in 24 h of reaction time. The silver nanoparticles recycled easily by simple centrifugation of the reaction mixture and used up to six times with a small decrease in the reactivity. The synergistic effect of Silver and Titania has advantages over both homogeneous and heterogeneous photocatalyst for the Suzuki-coupling reaction.

Acknowledgments

The authors are grateful for the financial support provided by the National Key Research and Development Program of China (No. 2017YFC040470002) and Guangdong Provincial

Natural Science Fund (No. 2017A030313321).

References

- [1] E. Negishi, Palladium-or nickel-catalyzed cross-coupling. A new selective method for carbon-carbon bond formation, *Acc. Chem. Res.*, 15 (1982) 340-348.
- [2] S.R. Chemler, D. Trauner, S.J. Danishefsky, The B- Alkyl Suzuki–Miyaura Cross-Coupling Reaction: Development, Mechanistic Study, and Applications in Natural Product Synthesis, *Angew. Chem. Int. Ed.*, 40 (2001) 4544-4568.
- [3] D. Pizzirani, M. Roberti, M. Recanatini, Domino Knoevenagel/Diels–Alder sequence coupled to Suzuki reaction: a valuable synthetic platform for chemical biology, *Tetrahedron Lett.*, 48 (2007) 7120-7124.
- [4] D. Howard Fairbrother, X.D. Peng, R. Viswanathan, P.C. Stair, M. Trenary, J. Fan, Carbon-carbon coupling of methyl groups on Pt(111), *Surf. Sci. Lett.*, 285 (1993) L455-L460.
- [5] R.J. Lundgren, M. Stradiotto, Addressing Challenges in Palladium- Catalyzed Cross-Coupling Reactions Through Ligand Design, *Chem. Eur. J.*, 18 (2012) 9758-9769.
- [6] D. Kalyani, N.R. Deprez, S. V. Desai, M.S. Sanford, Oxidative C–H activation/C–C bond forming reactions: synthetic scope and mechanistic insights, *J. Am. Chem. Soc.*, 127 (2005) 7330-7331.
- [7] P.D. Stevens, G. Li, J. Fan, M. Yen, Y. Gao, Recycling of homogeneous Pd catalysts using superparamagnetic nanoparticles as novel soluble supports for Suzuki, Heck, and Sonogashira cross-coupling reactions, *Chem. Commun.*, (2005) 4435-4437.
- [8] B. Giese, J.A. González- Gómez, T. Witzel, The Scope of Radical C–C Coupling by the “Tin Method”, *Angew. Chem. Int. Ed. Engl.*, 23 (1984) 69-70.

- [9] L. Celewicz, Photochemical coupling of 5-bromo-1,3-dimethyluracil and its 6-alkyl derivatives to 3-methylindole and *N*-acetyl-L-tryptophan methyl ester, *J. Photochem. Photobiol.*, B 3 (1989) 565 - 574.
- [10] P. Forgione, M.-C. Brochu, M. St-Onge, K.H. Thesen, M.D. Bailey, F. Bilodeau, Unexpected intermolecular Pd-catalyzed cross-coupling reaction employing heteroaromatic carboxylic acids as coupling partners, *J. Am. Chem. Soc.*, 128 (2006) 11350-11351.
- [11] C.-J. Li, Cross-dehydrogenative coupling (CDC): exploring C–C bond formations beyond functional group transformations, *Acc. Chem. Res.*, 42 (2008) 335-344.
- [12] J. Wang, P. Yang, B. Cao, J. Zhao, Z. Zhu, Photocatalytic carbon–carbon bond formation with concurrent hydrogen evolution on the Pt/PtO₂ nanotube, *Appl. Surf. Sci.*, 325 (2015) 86-90.
- [13] X.-H. Li, M. Baar, S. Blechert, M. Arconetti, Facilitating room-temperature Suzuki coupling reaction with light: Mott-Schottky photocatalyst for C–C-coupling, *Sci. Rep.*, 3 (2013) 1743.
- [14] Z.J. Wang, S. Ghasimi, K. Landfester, K.A. Zhang, Photocatalytic Suzuki coupling reaction using conjugated microporous polymer with immobilized palladium nanoparticles under visible light, *Chem. Mater.*, 27 (2015) 1921-1924.
- [15] Q. Xiao, S. Sampa, E. Jaatinen, J. Jia, D.P. Arnold, H. Liu, H. Zhu, Efficient photocatalytic Suzuki cross-coupling reactions on Au–Pd alloy nanoparticles under visible light irradiation, *Green Chem.*, 16 (2014) 4272-4285.
- [16] Z. Jiao, Z. Zhai, X. Guo, X.-Y. Guo, Visible-Light-Driven Photocatalytic Suzuki–Miyaura Coupling Reaction on Mott–Schottky-type Pd/SiC Catalyst, *J. Phys. Chem. C*, 119 (2015) 3238-3243.

- [17] D. Sun, Z. Li, Double-solvent method to Pd nanoclusters encapsulated inside the cavity of NH₂-Uio-66 (Zr) for efficient visible-light-promoted Suzuki coupling reaction, *J. Phys. Chem. C*, 120 (2016) 19744-19750.
- [18] Q. Xiao, S. Sarina, A. Bo, J. Jia, H. Liu, D.P. Arnold, Y. Huang, H. Wu, H. Zhu, Visible Light-Driven Cross-Coupling Reactions at Lower Temperatures Using a Photocatalyst of Palladium and Gold Alloy Nanoparticles, *ACS Catal.*, 4 (2014) 1725-1734.
- [19] M. Koohgard, M. Hosseini-Sarvari, Enhancement of Suzuki-Miyaura coupling reaction by photocatalytic palladium nanoparticles anchored to TiO₂ under visible light irradiation, *Catal. Commun.*, 111 (2018) 10-15.
- [20] L. Cermenati, A. Albin, C. Richter, Solar light induced carbon-carbon bond formation via TiO₂ photocatalysis, *Chem. Commun.*, (1998) 805-806.
- [21] M. Pirtsch, S. Paria, T. Matsuno, H. Itoh, J. Reiser, [Cu(dap)₂Cl] As an Efficient Visible- Light- Driven Photoredox Catalyst in Carbon-Carbon Bond- Forming Reactions, *Chem. Eur. J.*, 18 (2012) 7336-7340.
- [22] D. Yim, F. Raza, J.H. Park, J.H. Lee, H.I. Kim, J.K. Yang, I.J. Hwang, J.H. Kim, Ultrathin WO₃ Nanosheets Converted from Metallic WS₂ Sheets by Spontaneous Formation and Deposition of PdO Nanoclusters for Visible Light-Driven C-C Coupling Reactions, *ACS Appl. Mater. Interfaces*, 11 (2019) 36960-36969.
- [23] N. Wang, L.X. Ma, J. Wang, Y.P. Zhang, R.B. Jiang, Graphitic Carbon Nitride (g-C₃N₄) Supported Palladium Species: An Efficient Heterogeneous Photocatalyst Surpassing Homogeneous Thermal Heating Systems for Suzuki Coupling, *Chempluschem*, 84 (2019) 1164-1168.
- [24] M. Sahoo, S. Mansingh, S. Subudhi, P. Mohapatra, K. Parida, A plasmonic AuPd bimetallic nanoalloy decorated over a GO/LDH hybrid nanocomposite via a green synthesis

route for robust Suzuki coupling reactions: a paradigm shift towards a sustainable future, *Catal. Sci. Technol.*, 9 (2019) 4678-4692.

[25] A. Elhampour, F. Nemati, M.M. Heravi, Nano Ag-doped magnetic-Fe₃O₄@mesoporous TiO₂ core-shell hollow spheres: synthesis and enhanced catalytic activity in A(3) and KA(2) coupling reactions, *Monatsh. Chem.*, 148 (2017) 1793-1805.

[26] K. Sharma, M. Kumar, V. Bhalla, Aggregates of the pentacenequinone derivative as reactors for the preparation of Ag@Cu₂O core-shell NPs: an active photocatalyst for Suzuki and Suzuki type coupling reactions, *Chem. Commun.*, 51 (2015) 12529-12532.

[27] S. Gao, N. Shang, C. Feng, C. Wang, Z. Wang, Graphene oxide-palladium modified Ag-AgBr: a visible-light-responsive photocatalyst for the Suzuki coupling reaction, *RSC Adv.*, 4 (2014) 39242-39247.

[28] P.K. Prajapati, A. Kumar, S.L. Jain, First photocatalytic synthesis of cyclic carbonates from CO₂ and epoxides using CoPc/TiC₂ hybrid under mild conditions, *ACS Sustain. Chem. Eng.*, 6 (2018) 7799-7809.

[29] V.S. Manikandan, A.K. Palai, S. Mohanty, S.K. Nayak, Eosin-Y sensitized core-shell TiO₂-ZnO nano-structured photoanodes for dye-sensitized solar cell applications, *J. Photochem. Photobiol., B* 182 (2018) 397-404.

[30] B. Paul, B. Bhuyon, D.D. Purkayastha, S.S. Dhar, Photocatalytic and antibacterial activities of gold and silver nanoparticles synthesized using biomass of *Parkia roxburghii* leaf, *J. Photochem. Photobiol., B* 154 (2016) 1-7.

[31] V. Augugliaro, S. Coluccia, V. Loddo, L. Marchese, G. Martra, L. Palmisano, M. Schiavello, Photocatalytic oxidation of gaseous toluene on anatase TiO₂ catalyst: mechanistic aspects and FT-IR investigation, *Appl. Catal. B*, 20 (1999) 15-27.

[32] R. Gao, Y. Lu, S. Xiao, J. Li, Facile Fabrication of Nanofibrillated Chitin/Ag₂O Heterostructured Aerogels with High Iodine Capture Efficiency, *Sci. Rep.*, 7 (2017) 4303.

- [33] W. Wang, Z. Wang, J. Liu, Z. Luo, S.L. Suib, P. He, G. Ding, Z. Zhang, L. Sun, Single-step one-pot synthesis of TiO₂ nanosheets doped with sulfur on reduced graphene oxide with enhanced photocatalytic activity, *Sci. Rep.*, 7 (2017) 46610.
- [34] B. Bhuyan, A. Paul, B. Paul, S.S. Dhar, P. Dutta, *Paederia foetida* Linn. promoted biogenic gold and silver nanoparticles: Synthesis, characterization, photocatalytic and in vitro efficacy against clinically isolated pathogens, *J. Photochem. Photobiol., B* 173 (2017) 210–215.
- [35] M.J. Khan, K. Shameli, A.Q. Sazili, J. Selamat, S. Kumari, Rapid Green Synthesis and Characterization of Silver Nanoparticles Arbitrated by Curcumin in an Alkaline Medium, *Molecules*, 24 (2019) 719.
- [36] L. Stagi, C.M. Carbonaro, R. Corpino, D. Chiriac, P.C. Ricci, Light induced TiO₂ phase transformation: correlation with luminescent surface defects, *Phys. Status Solidi B*, 252 (2015) 124-129.
- [37] S. Porto, P. Fleury, T. Damen, Raman spectra of TiO₂, MgF₂, ZnF₂, FeF₂, and MnF₂, *Phys. Rev.*, 154 (1967) 522.
- [38] M. Gotić, M. Ivanda, S. Popović, S. Musić, A. Sekulić, A. Turković, K. Furić, Raman investigation of nanosized TiO₂, *J. of Raman Spectrosc.*, 28 (1997) 555-558.
- [39] H.C. Choi, Y.M. Jung, S.B. Kim, Size effects in the Raman spectra of TiO₂ nanoparticles, *Vib. Spectrosc.*, 37 (2005) 33-38.
- [40] B. Paul, S. Vadivel, N. Yadav, S.S. Dhar, Room temperature catalytic reduction of nitrobenzene to azoxybenzene over one pot synthesised reduced graphene oxide decorated with Ag/ZnO nanocomposite, *Catal. Commun.* 124 (2019) 71-75.
- [41] D. Hariharan, P. Thangamuniyandi, A.J. Christy, R. Vasantharaja, P. Selvakumare, S. Sagadevan, A. Pugazhendhi, L.C. Nehru, Enhanced photocatalysis and anticancer activity of

green hydrothermal synthesized Ag@TiO₂ nanoparticles, J. Photochem. Photobiol., B 202 (2020) 111636.

[42] M.A. Ahmed, Z.M. Abou-Gamra, H.A.A. Medien, M.A. Hamza, Effect of porphyrin on photocatalytic activity of TiO₂ nanoparticles toward Rhodamine B photodegradation, J. Photochem. Photobiol., B 176 (2017) 25–35.

[43] X. Gao, R.J. Esteves, T.T.H. Luong, R. Jaini, I.U. Arachchige, Oxidation-induced self-assembly of Ag Nanoshells into transparent and opaque Ag hydrogels and aerogels, J. Am. Chem. Soc., 136 (2014) 7993-8002.

[44] R. Sedghi, F. Heidari, A novel & effective visible light-driven TiO₂/magnetic porous graphene oxide nanocomposite for the degradation of dye pollutants, RSC Adv., 6 (2016) 49459-49468.

[45] D. Zhang, S. Cui, J. Yang, Preparation of Ag₂O/g-C₃N₄/Fe₃O₄ composites and the application in the photocatalytic degradation of Rhodamine B under visible light, J. Alloys Compd., 708 (2017) 1141-1149.

[46] P. Verma, Y. Kuwahara, K. Mori, H. Yamashita, Pd/Ag and Pd/Au bimetallic nanocatalysts on mesoporous silica for plasmon-mediated enhanced catalytic activity under visible light irradiation, J. Mater. Chem. A, 4 (2016) 10142-10150.

[47] A. Dawson, P.V. Yamat, Semiconductor– metal nanocomposites. Photoinduced fusion and photocatalysis of gold-capped TiO₂(TiO₂/gold) nanoparticles, J. Phys. Chem. B, 105 (2001) 960-966.

[48] U. Siemon, D. Bahnemann, J.J. Testa, D. Rodríguez, M.I. Litter, N. Bruno, Heterogeneous photocatalytic reactions comparing TiO₂ and Pt/TiO₂, J. Photochem. Photobiol. A, 148 (2002) 247-255.

[49] H. Einaga, T. Ibusuki, S. Futamura, Improvement of catalyst durability by deposition of Rh on TiO₂ in photooxidation of aromatic compounds, *Environ. Sci. Technol.*, 38 (2004) 285-289.

[50] J. Fu, S. Cao, J. Yu, Dual Z-scheme charge transfer in TiO₂-Ag-Cu₂O composite for enhanced photocatalytic hydrogen generation, *J. Materiomics*, 1 (2015) 124-133.

Journal Pre-proof

Author statement

All the authors performed the experiment and have successfully written the manuscript. All the authors contributed equally.

Journal Pre-proof

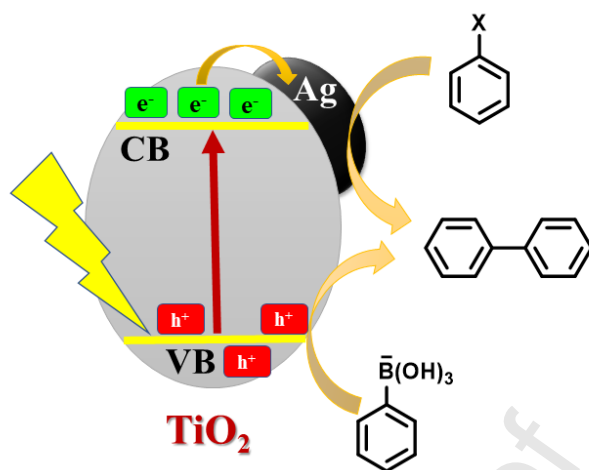
Declaration of interests

The authors declare that they have no known competing financial interests or personal relationships that could have appeared to influence the work reported in this paper.

The authors declare the following financial interests/personal relationships which may be considered as potential competing interests:

Journal Pre-proof

Graphical abstract



Highlights

- One-pot hydrothermal synthesis of silver supported titanium oxide.
- 2-5 nm Ag-nanoparticles supported on 20-50 nm TiO₂ nanoparticles.
- Photocatalytic Suzuki-coupling of bromoaryl with phenylboronic acid.
- 98% conversion of p-ethyl bromobenzene with a 97% yield of p-ethyl biphenyl.
- The photocatalyst is highly recyclable and can be used up to seven times.

Journal Pre-proof